Bull. Disas. Prev. Res. Inst., Kyoto Univ., Vol. 42, Part 2, No. 366, June, 1992

Three Dimensional Assimilation of Tropical Wind Field by MASCON Model

By Yurie HETA

(Manuscript received on April 1, 1992 ; revised on April. 27, 1992)

Abstract

Assimilation of tropical wind fields was developed using the three-dimensional Mass Consistent Atmospheric Flux (MASCON) model based on Sasaki's variational method[1]. Variational calculus techniques are used to adjust the spatially sparse wind data set of satellite cloud and rawinsonde, satisfying the continuity equation. Three-dimensional wind fields (u, v, ω) are provided over the whole troposphere using the p coordinate, which is a hybrid of the p and σ - coordinates. This model can give us a three-dimensional wind field in the tropical region for the analysis of synoptic scale phenomena.

Reanalysis of the tropical wind field surrounding tropical disturbances reveals characteristics similar to the previous two-dimensional MASCON model (Heta[2)3)]). Moreover vertical velocity can be calculated directly in the three-dimensional model. As a result, an upward motion area is recognized around a pre-typhoon disturbance with upward velocity increasing with the development of the disturbance.

1. Introduction

In areas with sparse observational data such as over the tropical Pacific Ocean, the data should be assimilated before applying advanced analysis technics or prognostic computation. The global scale assimilation systems have been developed by the European Centre for Medium Range Weather Forecasts (ECMWF), the Geophysical Fluid Dynamics Laboratory (GFDL) and others using governing equations of motion (Bengtsson et al[4], Lorenc[5], Daley et al[6], Trenberth et al[7]). And many researchers have analyzed the tropical wave disturbance using gridded wind fields assimilated by these methods (e. g. Nitta and Takayabu[8], Lau and Lau[9] and Liebmann and Hendon[10]).

The purpose of this paper is to describe a new simple three dimensional assimilation method for equatorial wind field following MASCON method to obtain $1^\circ \times 1^\circ$ mesh wind field from station and satellite cloud wind information, which is an extension of a two dimensional method developed by the present author (Heta[2]).

2. Model description

Based on Sasaki's variational method[1], Dickerson[11] developed a two-dimensional MASCON model using the equation of continuity as the constraint condition, which the first

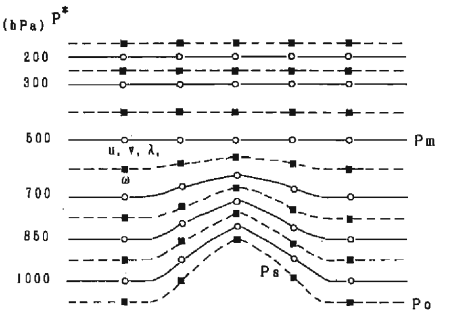

Fig. 1. Vertical grid structure of the model. Solid lines show main levels (○ — u, v, λ and ■ — ω).

model of the present author (Heta[2]) had also followed. In extending the model into three-dimensions, there may be various kinds of vertical coordinates for numerical calculation, as shown by Kasahara[12]. The simplest one is the z-coordinate used by Sherman[13] who developed the mass-adjusted three-dimensional wind field (MATHEW) model for lower troposheric wind fields over a complex terrain. The present system has adopted the pressure coordinate p^* to include the whole troposphere of an equatorial area defined by

$$p^* = \begin{cases} (p_o - p_m) * (p_m - p)/(p_m - p_s) + p_m & (p \geq p_m) \\ p & (p < p_m) \end{cases} \tag{1}$$

where p_s is the surface pressure. As shown in **Fig. 1,** only the layers below p_m are affected by the orography, which is relatively low in the tropics. p_m is decided as a constant value (in this case, p_m=500hPa). This coordinate is a hybrid of p-coordinate and σ-coordinate, and is chosen to incooperate the topography of the tropical Pacific in the model, where the highest point is about 700hPa in New Guinea.

In this coordinate, we define the time change of p^* as

$$\omega^* = dp^*/dt = (p_o - p_m) \times (\omega - v \cdot \nabla_{p*} p)/(p_s - p_m) \tag{2}$$

where $\omega = dp/dt$.

Then the continuity equation in the (x, y, p^*) coordinate becomes,

$$\partial(\varepsilon u)/\partial x + \partial(\varepsilon v)/\partial y + \partial(\varepsilon \omega^*)/\partial p^* = 0 \tag{3}$$

where,

$$\varepsilon = \begin{cases} (p_s - p_m)/(p_o - p_m) & (p \geq p_m) \\ 1 & (p < p_m) \end{cases} \tag{4}$$

As p^* is basically a pressure coordinate, the whole troposphere can be handled without assumptions about air density.

Even though the pressure of the ground surface, p_s(hPa) is strictly a function of time,

fixed values are used in this study following climatological relations with heights in the tropical atmosphere given by

$$p_s=1016.17\{\exp(-0.11746* z_s)-1\}+p_o \tag{5}$$

where p_o is a constant pressure and z_s is an altitude of the land (m) at each grid point. The specific functional of three-dimensional variational analysis (Sasaki[1]) used in the present study is

$$E(u, v, \omega^*, \lambda)=\int \{\{\alpha_1^2(u-\tilde{u})^2+\alpha_1^2(v-\tilde{v})^2+\alpha_2^2(\omega^*-\tilde{\omega}^*)^2\}+ \lambda(\partial u/\partial x+\partial v/\partial y+\partial\omega^*/\partial p^*)\}dxdydp^* \tag{6}$$

where x, y are horizontal coordinates, u, v, ω^* adjusted velocity components in the x, y, p^* directions respectively, $\tilde{u}, \tilde{v}, \tilde{\omega}^*$ the observed variables, $\lambda(x, y, p^*)$ the Lagrange multiplier and α_k being Gaussian precision moduli for horizontal ($k=1$) and vertical ($k=2$) directions.

The associated Euler-Lagrange equations whose solution minimizes Eq. (6) are,

$$u=\tilde{u}+1/(2\alpha_1^2\gamma)\cdot\partial\lambda/\partial x \tag{7}$$
$$v=\tilde{v}+1/(2\alpha_1^2\gamma)\cdot\partial\lambda/\partial y \tag{8}$$
$$\omega^*=\tilde{\omega}^*+1/(2\alpha_2^2\gamma)\cdot\partial\lambda/\partial p^* \tag{9}$$
$$\partial u/\partial x+\partial v/\partial y+\partial\omega^*/\partial p^*=0 \tag{10}$$

The bottom and upper boundary condition is $\partial\lambda/\partial n=0$, which means "noflow-through" boundaries, while the lateral, on the x-direction and y-direction, boundary condition is open boundary or $\lambda=0$.

In this formulation, from the initial wind field $(\tilde{u}, \tilde{v}, \tilde{\omega}^*)$ at each grid point, we can obtain an adjusted wind field (u, v, ω^*), which satisfies the continuity equation and also fits the observation in a least squares manner, using MASCON model. In this process, it is important to interpolate the proper initial wind field $(\tilde{u}, \tilde{v}, \tilde{\omega}^*)$ from the observation. In the next section, the interpolation method is described in detail.

3. Interpolation method

Randomly distributed observations must be spatially interpolated to the grid points as the initial condition to apply the MASCON model. Since measurement of the vertical velocity ω is not available, by observation, it is initially set to zero, similar to the MATHEW model. Initial values of u and v at the grid point (x, y, p) above p_m (500hPa) level were prepared in a two-dimensional interpolation scheme without respect to adjustment layer similar to that of Dickerson[11], shown as follows,

$$V_i=\sum_{j=1}^{N} SV_{ij}\ \exp(-\beta r_j^2)/\sum_{j=1}^{N} S\exp(-\beta r_j^2) \tag{11}$$

where V_i is the interpolated east-west(i=1) or north-south(i=2) velocity component at the

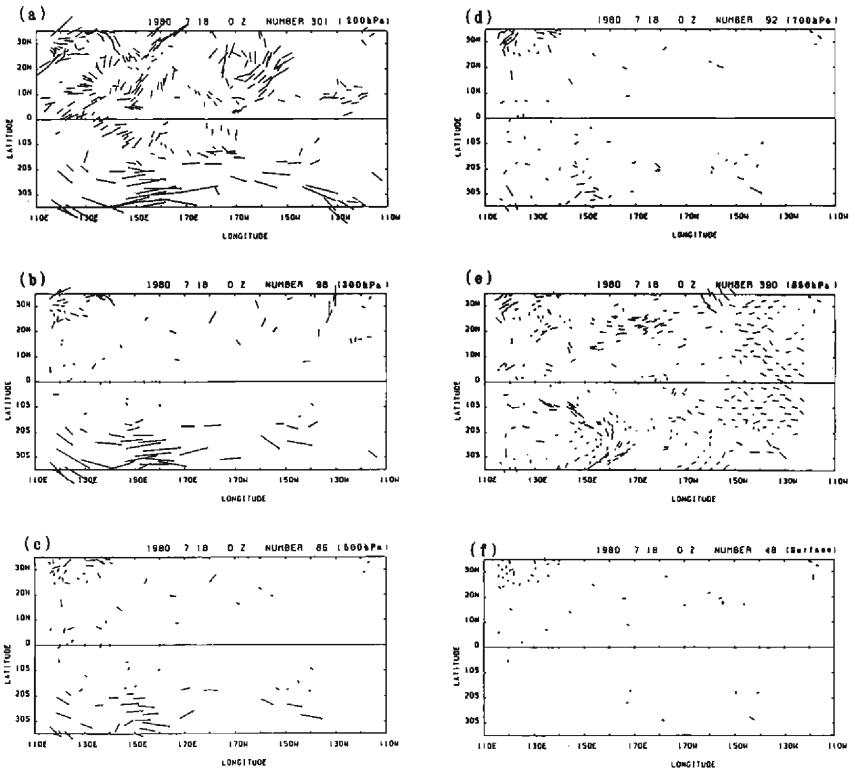

Fig. 2. Distribution of observational wind data at (a) 200hPa, (b) 300hPa, (c) 500hPa, (d) 700hPa, (e) 850hPa and (f) 1000hPa levels at 00Z on 18 July, 1980.

grid point; V_{ij} and r_j are the i–th velocity component and distance in meter to the grid point of the j–th closest observation, and N is the number of the closest observations to the grid point that are used for interpolation. β is the weight depending on horizontal distance being 10^{-12} or the same as the previous two– dimensional MASCON model(Heta[2)3)]). For this study we have chosen a value of 5 for N which is usual. In addition, we have added the weight, S, which varies with the kind of observation. After several trials changing S, we decided $S=1$ for sonde and $S=0.9$ for satellite wind data. In **Fig. 2,** there is a typical distribution of wind observations. The satellite winds are included in the 850hPa and 200hPa layers following the results of comparison with the rawinsonde data(Hamada[14)]).

Below the layer of p_m, we adopted a three–dimensional interpolation. Therefore, the distance of the grid point of the j–th closest observation, r_j in eq(11) is given by

$$r_j^2=(x-\tilde{x}_{oj})^2+(y-\tilde{y}_{oj})^2+(p^*-\tilde{p}_{oj})^2\times Wz^2 \qquad (12)$$

where $\tilde{x}_{oj}$, $\tilde{y}_{oj}$, $\tilde{p}_{oj}$ is the position of j–th nearest observational point. Wz is the vertical weight to represent the heterogeneousness of the vertical coordinate. The vertical weight Wz has much effect on the resultant wind fields especially for layers of sparse data, such as 1000hPa

or 700hPa. If the value of Wz is tends to large, the interpolation is horizontal, but if it is small, the resulting wind fields show more similar patterns for all layers. After several trials, the value of Wz was set as 50(m/Pa) for all layers below p_m, which minimizes the root mean square difference between observational wind and interpolated wind at the nearest grid point. The values of root mean square differences are about 2~5m/s for the case of $Wz=50$.

The interpolation stated above is quite dependent on the wind data of the adjacent observations. We examined a possibility to improve the interpolated wind field by using the data at the previous time especially in the data sparse areas, such as the case where only m($<N$) observations existed within a certain radius of r_m. In this test case the adjusted wind data at the previous time, Vpi at the same grid point was used for the interpolation;

$$Vri=\frac{m+N-1}{2N}\frac{\sum_{j=1}^{N} V_{ij}\, S\exp(-\beta r_j^2)}{\sum_{j=1}^{N} S\exp(-\beta r_j^2)}+\frac{m-N-1}{2N}\,Vpi \tag{13}$$

However, this treatment had little significant effect on the results because data was also sparse at the previous time for many cases of 24-hour interval calculation. Only for the cases where the data density was high at the previous time, was this treatment useful. However, in the present paper, this process is not used except for those cases where the observation is quite poor compared with the previous day. Since 1987, the satellite wind data have been provided four times a day, though, rawinsonde data are still available only once or twice a day. For the analysis of six hourly wind fields, this interpolation scheme may be useful.

Fig. 3 shows an example of the distribution of a number of observational points ($\leq N$) within a radius of $r_m=10^\circ$ (1100km) from the grid point for 18 July, 1980. The regions of a low number such as centered at 170W, ON(**Fig. 3(a)**) have lower data accuracy compared with the region where the number is five($=N$). Data sparse areas are often located along the equator where there are no islands and less clouds.

The interpolated wind field is quite influenced by bad data. A data quality check was performed for every case by plotting all the data on maps. If bad data was revealed, which had improper direction or speed, such data was omitted and not used for interpolation.

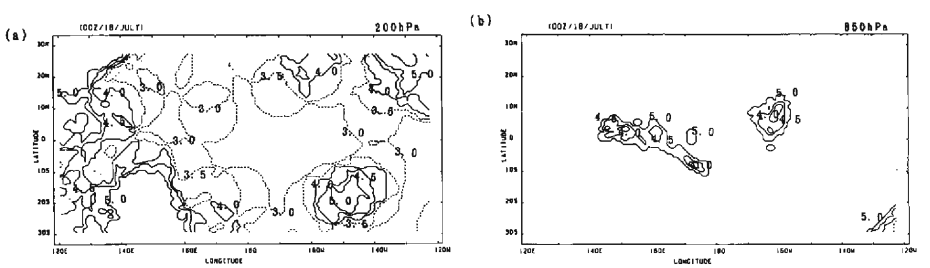

Fig. 3. Numbers of observational points which are located in the radius of 10° longitude (10×110km) at each grid point at (a) 200hPa and (b) 850hPa levels at 0Z on 18 July, 1980. Contour interval is 0.5. Contours of five (=N) and below are shown.

4. Parameters in the MASCON model.

The ratio of Gaussian precision moduli $(\alpha_1/\alpha_2)^2$ in eq(6) affects the resulting wind field very much, though there is no clearly formulated way to determine the value. In the present paper, we determined the value of $(\alpha_1/\alpha_2)^2$ after similar trials as in the previous study (Heta[3]), where $\alpha_1/\alpha_2=0.08$, which minimizes the absolute error from continuity equation, ε (Sasaki[1]).

The absolute value of adjusted ω were also dependent on the ratio of α's because the observational $\tilde{\omega}$ was set to be zero in the present study. If smaller values of α_1/α_2 are chosen, the absolute value of the resulting ω becomes smaller. However, comparing the distribution of ω values, the horizontal and vertical pattern of ω is independent of the ratio of α's.

The overrelaxation factor was determined experimentally to be 1.98 in most calculations minimizing the calculation time. All the parameters were determined experimentally for the case of July, 1980. The area has $120\times60\times6$ grid points, $\Delta x=\Delta y=110$km and six layers (1000hPa, 850hPa, 700hPa, 500hPa, 300hPa and 200hPa), but Δp is not constant. The analyzed area covers 120E~120W, 30S~30N. The data of July, 1980 were chosen to compare with the previous result (Heta[2)3)]). **Fig. 4** shows the topography of the analyzed area.

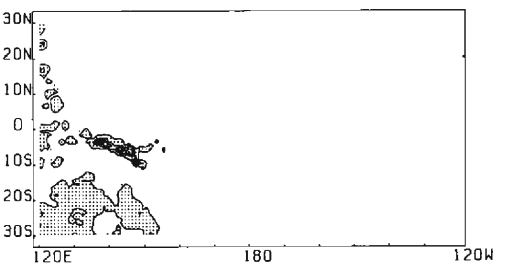

Fig. 4. Topography of the analyzed region. Contour interval is 500m.

5. Results

The adjusted three-dimensional MASCON model has been applied to assimilation of the wind field of July, 1980. **Fig. 5** shows the results of the horizontal wind fields at the 200hPa and 850hPa levels at 0Z on 18 July, 1980. A tropical depression was located as 13.4N, 138.9E at this time, which later developed into Typhoon Joe. There is a cyclonic circulation around the tropical depression at 850hPa level (**Fig. 5(a)**). The south-east of the tropical depressions northward current across the equator and easterly winds are converging. At 200hPa level (**Fig. 5(b)**), on the other hand, anticyclonic outflow toward the west is clearly seen a little east of the location of tropical depression. There are counter-clockwise circulations centered at 20N, 170W and at 5S, 173E. We recognized strong southwesterlies around 160W, 20N, which are thought to be a current along the edge of Mid-Pacific Trough. The horizontal wind fields at the 850hPa and 200hPa levels, such as shown in **Figs. 5(a)** and **(b)**, are almost

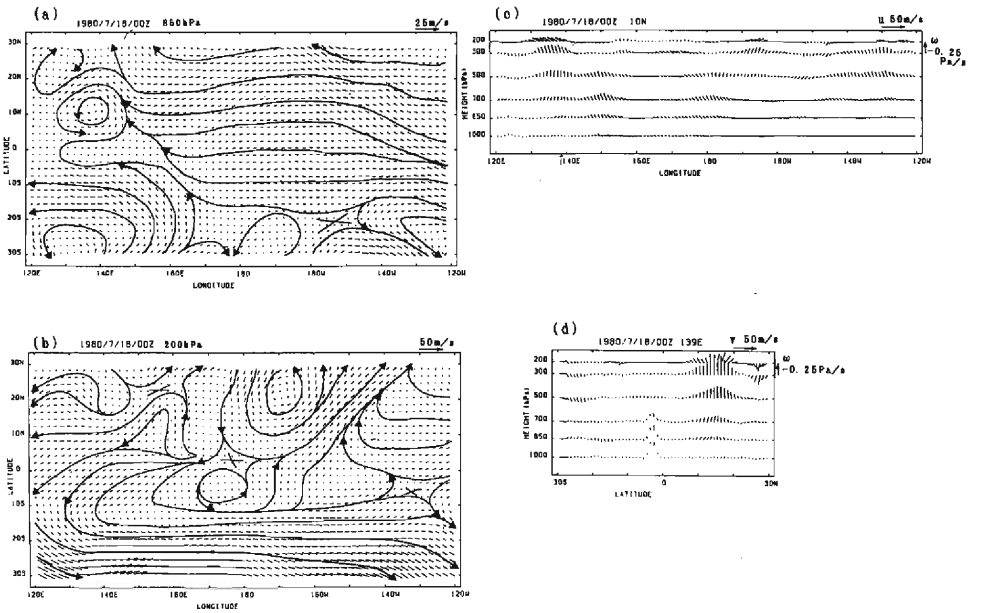

Fig. 5. (a) Horizontal wind field at the 850hPa level adjusted by the three-dimensional MASCON model at 0Z on 18 July, 1980.

(b) As in (a), except for 200hPa level.

(c) Vertical-longitudinal structure along 10N zone.

(d) Vertical-latitudinal structure along 139E. Upward arrows indicate negative values of ω.

similar to the result from the previous two-dimensional analysis (not shown). **Fig. 5(c)** shows longitude-height section at 10N, and **Fig. 5(d)** latitude-height section at 139E. Strong upward motion is recognized around the tropical depression in both figures. ω shows its maximum value at 500hPa or 300hPa levels. The absolute value of ω at lower levels is small compared with the upper levels and the distribution of ω is quite smooth compared with upper ones.

Fig. 6 shows the distribution of ω at 200hPa and cloud activity, which is shown as the T_{BB} anomaly from the monthly mean value. They are in good coincidence with each other. The upward motion area corresponds to the T_{BB} negative anomalous area, that is the area of higher cloud activity compared with the monthly mean state. The upward motion area is recognized around the areas centered at 138E, 15N and 160E, 5N in **Fig. 6(a)**. These locations coincide with the area of horizontal divergence at the 200hPa level in the previous two dimensional analysis (Heta[2], **Fig. 7(a)**).

Fig. 7 shows the results of analysis of Typhoon 8009 using the three-dimensional MASCON model. The broken line with small open circles indicates the track of pre-typhoon disturbance, which is defined by the mean positions of lower convergence and positive vorticity, and upper divergence and negative vorticity regions just the same as the two

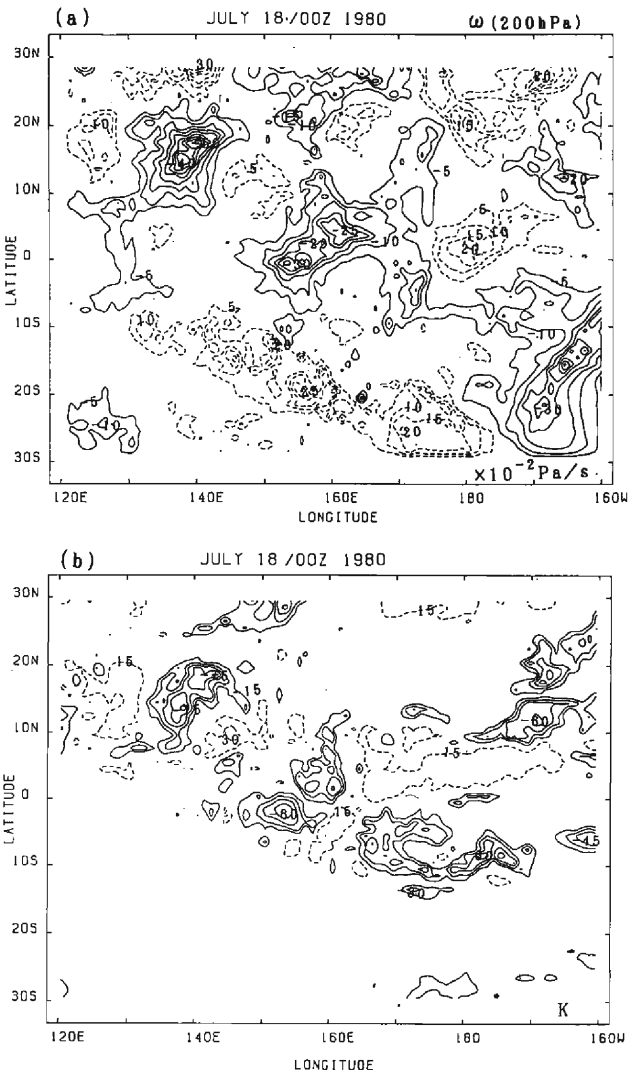

Fig. 6. (a) The distribution of ω values at the 200hPa level at 0Z on 18, July, 1980. Solid lines show the negative values and broken lines show the positive values. Contour interval is 0.05Pa/s.

(b) The distribution of anomaly of T_{BB} grid point data from the monthly mean values at 0Z on 18 July, 1980. Solid lines indicate the negative values and broken lines show the positive values. Contour interval is 15K.

dimensional MASCON model in the previous study (Heta[3], **Fig. 8**). **Fig. 7(b)** shows the negative ω regions of 200hPa of every other day. The upward motion area is also analyzed about the position of disturbace for other levels. **Fig. 7(a)** shows the positive ω regions. The subsidence motion is recognized around the upper positive vorticity area or the upper cold low.

Fig. 8 shows the time change of ω values for three-different levels at the center of

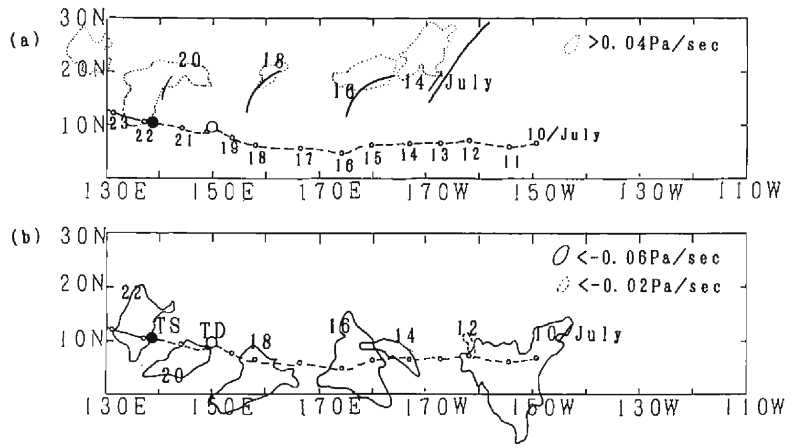

Fig. 7. (a) 200hPa positive vertical velocity regions at 0Z of every other day (dotted lines) and position of the axis and center of 200hPa positive vorticity regions (thick solid lines) analyzed in the previous study (Heta[3]). Small open circles with smaller numerals show the daily positions of tropical disturbances at 0Z from the previous two-dimensional analysis. Numerals mean day of July. Large open circle and large closed circle indicate the positions where the disturbances had Tropical Depression and Tropical Storm intensity, respectively.

(b) Position of 200hPa negative ω regions (thick solid lines) at 0Z of every other day.

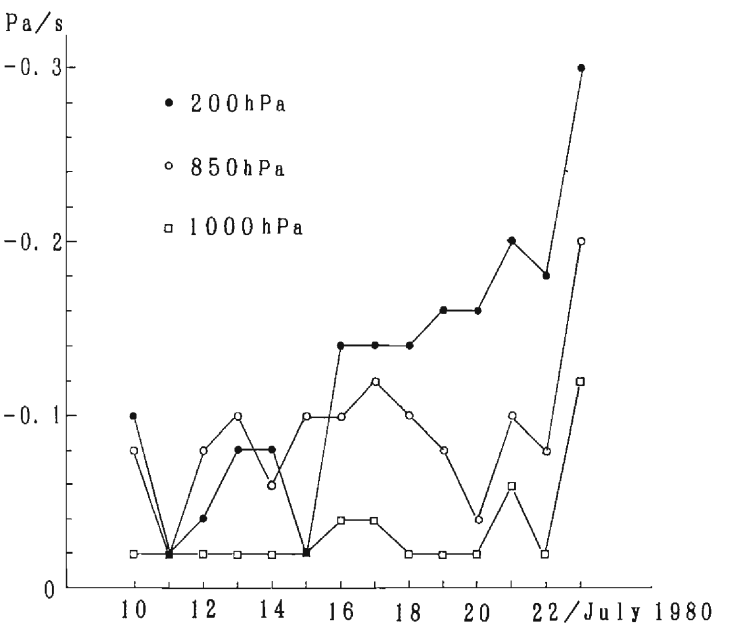

Fig. 8. Time change of the ω values at 200hPa, 850hPa and 1000hPa levels at the center of the wave disturbances detected by the previous analysis.

Typhoon 8009. The development of the typhoon is recognized by the change of ω value, though small changes of the values may come from noises caused by the change of accuracy of analysis.

These figures show that the pre-typhoon disturbances or the upper cold low analyzed by the previous two-dimensional study are also analyzed by the three-dimensional MASCON model. Moreover we can directly ascertain the vertical motion of disturbances by this three-dimensional study.

6. Conclusion

The assimilation method using the three-dimensional MASCON model provides us with tropical wind fields which enable us analyze tropical disturbances in more detail than the two dimensional method (Heta[2)3)]). The vertical velocity is directly obtained in this model. The three-dimensional wind fields adjusted in a least-squares sense to satisfy the continuity equation are provided.

Reanalysis of the Typhoon 8009 using the three-dimensional MASCON model indicates similar characterisitics of the disturbance with the previous study by two-dimensional MASCON model for the same data. The results obtained in the previous papers by the simpler method of wind calculation, are shown to be true by the comparison of wind fields in the present paper. Moreover, vertical velocity is directly calculated in the present study. Upward motion (negative ω) areas are recognized around the pre-typhoon disturbance and value of ω decreased with the development of the disturbance.

Acknowledgements

The author expresses her thanks to Prof. Y. Mitsuta of Kyoto University for his continuous encouragement of this study. Thanks are due to Dr. T. Nakazawa of the Meteorological Research Institute, who kindly provided me with the NOAA OLR data and T_{BB} grid point data utilized in the present study. The author would also like to thank Prof. Y. K. Sasaki of Oklahoma Univ. and Dr. M. Murakami of the Meteorological Research Institute for their helpful comments and suggestions.

References

1) Sasaki, Y. K.: Lecture notes on variational methods for environmental analysis and prediction problems, *Severe Storm Research Notes.* 1, Disaster Prevention Research Institute, Kyoto University, 1979, 174pp.
2) Heta, Y.: An analysis of tropical wind fields in relation to typhoon formation over the western Pacific, *J. Meteor. Soc. Japan,* Vol. 68, 1990, pp. 65–77.
3) Heta, Y.: The origin of tropical disturbances over the equatorial Pacific, *J. Meteor. Soc. Japan,* Vol. 69, 1991, pp. 337–351.
4) Bengtsson, L., M. Kanamitsu, P. Kallberg and S. Uppala: FGGE 4-dimensional data assimulation at ECMWF, *Bull. Amer. Meteor. Soc.,* Vol. 63, 1982, pp. 29–43.
5) Lorenc, A. C.: A Global Three-dimensional Multivariate Statistical Interpolation Scheme, *Mon. Wea. Rew.,* Vol. 109, 1981, pp. 701–721.
6) Daley, R., A. Hollingsworth, J. Ploshay, K. Miyakoda, W. Banaley, C. Dey, T. Krishnamurti,

and E. Barker : Objective analysis and assimilation techniques used for the production of FGGE IIIb analyses, *Bull. Amer. Meteor. Soc.*, Vol. 66, 1985, pp. 532–538.

7) Trenberth, K. E. and J. G. Olson : An evaluation and intercomparison of global analyses from the National Meteorological Center and the European Centre for Medium Range Weather Forecasts, *Bull. Amer. Meteor. Soc.*, Vol. 69, 1988, pp. 1047–1057.

8) Nitta, T. and Y. Takayabu : Global analysis of the lower tropospheric disturbances in the tropics during the northern summer of the FGGE year part II : Regional characteristics of the disturbances, *PAGEOPH*, Vol. 123, 1985, pp. 272–292.

9) Lau, K. H. and N. C. Lau : Observed structure and propagation characteristics of tropical summertime synoptic scale disturbances, *Mon. Wea. Rev.*, Vol. 118, 1990, pp. 1888–1913.

10) Liebmann, B. and H. H. Hendon : Synoptic-scale disturbances near the equator, *J. Atmos. Soc.*, Vol. 47, 1990, pp. 1463–1479.

11) Dickerson, M. H. : MASCON–Mass Consistent Atmospheric Flux Model for regions with complex terrain, *J. Appl. Meteor.*, Vol. 17, 1978, pp. 241–253.

12) Kasahara. A : Various vertical coordinate systems used for numerical weather prediction, *Mon. Wea. Rev.*, Vol. 102, 1974, pp. 509–522.

13) Sherman, C. A. : A mass consistent model for wind fields over complex terrain, *J. Appl. Meteor.*, Vol. 17, 1978, pp. 312–319.

14) Hamada, T. : Representative heights of GMS satellite winds, *Meteorological Satellite Center Technical Note*, Vol. 6, 1982, pp. 35–47.